HHS Public Access

Author manuscript

J Am Coll Cardiol. Author manuscript; available in PMC 2018 January 24.

Published in final edited form as:

J Am Coll Cardiol. 2017 January 24; 69(3): 303–321. doi:10.1016/j.jacc.2016.10.065.

Wholly Patient-tailored Ablation of Atrial Fibrillation Guided by Spatio-Temporal Dispersion of Electrograms in the Absence of Pulmonary Veins Isolation

Julien Seitz, MD[*], **Clément Bars, MD**[*,y], **Guillaume Théodore, MD**[z], **Sylvain Beurtheret, MD**[*], **Nicolas Lellouche, MD, PHD**[x], **Michel Bremondy, MD**[*], **Ange Ferracci, MD**[*], **Jacques Faure**[*], **Guillaume Penaranda**[jj], **Masatoshi Yamazaki**[{], **Uma Mahesh R. Avula, MD**[{], **Laurence Curel, MS**[*], **Sabrina Siame**[*], **Omer Berenfeld, PHD**[{], **André Pisapia, MD**[*], and **Jérôme Kalifa, MD, PHD.**[{]

[*]St. Joseph Hospital, Marseille, France

[y]Private Hospital Institute Mutualiste Montsouris, Paris, France

[z]University Hospital, Nice, France

[x]Henri Mondor University Hospital, Creteil, France

[jj]Alphabio laboratory, Marseille, France

[{]University of Michigan, Ann Arbor, USA

Abstract

Background—The use of intra-cardiac electrograms to guide atrial fibrillation (AF) ablation has yielded conflicting results. We evaluated an electrogram marker of AF drivers: the clustering of electrograms exhibiting spatio-temporal dispersion — regardless of whether such electrograms were fractionated or not.

Address for Correspondence: Julien Seitz, MD, Hôpital Saint Joseph, Service de Cardiologie, 26 Bd de Louvain, 13008 Marseille, France, jseitz@hopital-saint-joseph.fr, Tel: +33491807044 Fax: +33491806925.

Disclosures

- Dr Seitz received speaker fees and honoraria as a consultant from Biosense Webster, speaker fees from St Jude Medical and Medtronic and owns shares of Volta medical.
- Dr Bars received speaker fees and honoraria as a consultant from Biosense Webster and owns shares of Volta medical.
- Dr Theodore received honoraria as a consultant from Biotronik, Boston Scientific, Saint Jude Medical and Medtronic.
- Pr Lellouche received speaker fees from Medtronic
- Drs Bremondy received honoraria from Saint Jude Medical within the STAR AF II trial study
- Drs Faure and Ferracci received honoraria from St Jude Medical as consultants.
- Dr. Berenfeld received grants and donations from Medtronic and St-Jude Medical, is a consultant for Acutus Medical, and holds shares from Rhythm Solutions.
- Dr Pisapia received honoraria as a consultant within the STAR AF II trial from Saint Jude Medical and speaker fees from Medtronic.
- Dr. Kalifa is co-investigator on a project sponsored by Medtronic and owns shares of Volta medical.

All other authors: None

Objective—To evaluate the usefulness of spatio-temporal dispersion, a visually recognizable electric footprint of AF drivers, for the ablation of all forms of AF.

Methods—We prospectively enrolled 105 patients admitted for AF ablation. AF was sequentially mapped in both atria with a 20-pole PentaRay catheter. We tagged and ablated only regions displaying electrogram dispersion during AF. Results were compared to a validation set in which a conventional ablation approach was used (pulmonary vein isolation/stepwise approach). To establish the mechanism underlying spatio-temporal dispersion of AF electrograms, we conducted realistic numerical simulations of AF drivers in a 2-dimensional model and optical mapping of ovine atrial scar-related AF.

Results—Ablation at dispersion areas terminated AF in 95%. After ablation of 17±10% of the left atrial surface and 18 months of follow-up, the atrial arrhythmia recurrence rate was 15% after 1.4±0.5 procedure/patient vs 41% in the validation set after 1.5±0.5 procedure/patient (arrhythmia free-survival rates: 85% vs 59%, log rank *P<0.001*). In comparison with the validation set, radiofrequency times (49 ± 21 minutes vs 85 ± 34.5 minutes, p=0.001) and procedure times (168 ± 42 minutes vs. 230 ± 67 minutes, p<.0001) were shorter. In simulations and optical mapping experiments, virtual PentaRay recordings demonstrated that electrogram dispersion is mostly recorded in the vicinity of a driver.

Conclusions—The clustering of intra-cardiac electrograms exhibiting spatio-temporal dispersion is indicative of AF drivers. Their ablation allows for a non-extensive and patient-tailored approach to AF ablation. *Clinical trial.gov number: NCT02093949*

Keywords

Atrial Fibrillation; Ablation; Dispersion; Mapping; Electrogram; Driver

Introduction

Visual appraisal of the sequence and morphology of intracardiac electrograms is sufficient to guide ablation of most ventricular and atrial arrhythmias. Atrial fibrillation (AF) is an exception to this paradigm. The targeting of complex fractionated electrograms (CFAEs) as a stand-alone or adjunctive ablation therapy has yielded variable results. (1–8) While some have reported good results when targeting CFAEs,(6–8) a growing number of reports shows that there is little advantage in targeting CFAEs after having isolated the PVs.(1–5) CFAEs ablation is usually guided by the recording of fractionated electrograms at the tip of a single intra-cardiac electrode. The added value that multipolar electrode-obtained CFAEs may provide over single electrode-recorded CFAEs has been suggested in multiple studies. Jais et al.,(9) Rostock et al.,(10) and Narayan et al.(11) demonstrated that multipolar electrode recordings during AF may enable a classification of CFAEs into “active” or “passive”. These authors have specifically pointed out that fractionation occurring in a non-simultaneous fashion at neighboring electrode locations (time dispersion) and organized in well-defined clusters (spatial dispersion) may indicate the presence of an underlying source of AF.(9–12) Recently, it was suggested that such multi-electrode electrogram clusters may be useful in guiding ablation.(11,13)

Sophisticated intracardiac electrogram analysis may enable the visualization of AF drivers. (14,15) It is unclear, however, whether multipolar electrogram signatures may be used as surrogates for the presence of drivers. Altogether, the usefulness of intra-cardiac electrograms for AF ablation remains uncertain. The purpose of this pilot study was to describe a visually recognizable intra-cardiac electrogram abnormality that can identify regions of AF drivers that are effective target sites for ablation of paroxysmal or persistent AF.

Methods

The hypothesis underlying this study is that electrograms recorded simultaneously by a multipolar catheter displaying *both* a spatial and temporal dispersion (dispersion areas) are indicative of AF drivers, regardless of whether or not these electrograms are fractionated. In Figure 1A, we present the typical feature of abnormal multipolar electrograms associated with AF drivers: the spatio-temporal dispersion of the electrical activation. Figure 1B and Figure 2 show examples of fractionated and non-fractionated single-bipole and multipolar electrograms recorded in dispersion regions.

Clinical study

Study population and validation set—Between September 2013 and July 2014, 126 patients with drug-refractory symptomatic AF were prospectively enrolled at three centers (Hopital St-Joseph, Marseille; Institut Mutualiste Monsouris; Paris and Centre Hospitalier Universitaire, Nice). Ablations were performed independently by seven electrophysiologists. The validation set included a cohort of patients with symptomatic drug-refractory AF who underwent ablation using a conventional approach (see below). From a database of 98 patients ablated conventionally (pulmonary vein isolation/stepwise approach) between November 2008 and March 2010, 47 controls were selected based on the following clinical characteristics at the time of the procedure: sex, presence of structural heart disease, and duration of continuous AF. The only exclusion criterion in the study and validation set was a prior AF ablation procedure. The study was approved by the institutional ethics committees and all patients provided signed informed consent.

Protocols—In the study population, only dispersion areas were ablated. The following catheters were introduced through the right femoral vein: (i) a deflectable decapolar catheter (2–5–2 mm electrode spacing, Biosense Webster, Diamond Bar, California, USA) positioned within the coronary sinus (CS); (ii) a deflectable multipolar catheter: PentaRay® NAv (20 poles, 4-4-4 mm electrode spacing, Biosense Webster, Inc. (iii) a 3.5 mm irrigated-tip quadripolar ablation catheter (Smart Touch, 2–5–2 mm inter-electrode spacing, D/F or F/J curves, Biosense Webster, Inc.). These catheters were introduced through a long sheath (Preface multipurpose, Biosense Webster, Inc.) and perfused with heparinized saline. Heparin was administered intravenously to maintain an activated clotting time in the 300–350 sec. range. Esophageal temperature was monitored during the procedure (esophageal probe, Sensitherm Saint-Jude Medical).

For patients in sinus rhythm (SR) at the outset of the procedure, AF was induced by rapid atrial pacing using the CS catheter (500–180ms). If AF was not inducible, isoproterenol

(baseline dose: 2.4 mg/h, increased in 0.2-mg increments in order to obtain a sinus rate > 100 bpm) was infused. A reference AF cycle length (AFCL) value was calculated as the average of two consecutive measurements of 10 CLs either in the left or right atrial (LA and RA) appendages (LAA and RAA, figure S1). See the online supplemental manuscript for details on the validation set ablation procedure.

Baseline mapping—Baseline mapping in both atria was performed during AF with a multispline catheter (PentaRay® NAv4-4-4 mm, Biosense Webster, Inc, Figure 1A). This multielectrode catheter was sequentially positioned in various regions of the RA and LA. At each location, the catheter was maintained in a stable position for a minimum of 2.5 sec (acquisition time window in CARTO). The operator looked for dispersion areas (electrograms exhibiting both time and spatial dispersion). In regions where dispersion was found and/or when the catheter was not in a stable position for 2.5 sec., acquisitions were repeated multiple times.

Dispersion areas were defined as clusters of electrograms, either fractionated or non-fractionated, that displayed inter-electrode time and space dispersion at a minimum of three adjacent bipoles such that activation spread over all the AF cycle length (Figure 1A and Figure 1B). At each bipole in a dispersion area, one or several of the following fractionated or non-fractionated electrogram morphologies were found Figure 1B): (i) continuous, low-voltage fractionated electrograms (“continuously fractionated signal”); (ii) bursts of fractionated electrograms (“trains of fractionation”). (iii) fast non-fractionated electrograms (AFCL < 120 ms; “rapid fires”); (iv) slow non-fractionated electrograms (AFCL> 120 ms). Four representative multipolar electrograms dispersion and non-dispersion regions are shown in Figure 2. These examples illustrate that fractionated electrograms (noted **f**) were found in both dispersion and non-dispersion regions.

Ablation protocol in the study group—We used a single transseptal sheath. Once the initial bi-atrial mapping with the PentaRay catheter was obtained, there was no further EGM analysis/evaluation performed either visually or quantitatively on electrograms recorded with the ablation catheter. The choice of the first dispersion region to ablate was left at the ablationist’s discretion. Retrospectively, ablationists indicated that they tended to start with the region that was seemingly activated at the fastest rate. Still, we have not conducted any “online” quantitative analysis of the frequency of activation in dispersion regions. Therefore, the operators’ impression will need to be rigorously evaluated in future studies.

RF energy was applied (10–45 W) at any atrial location including the PV antrum and the CS, while no ablation was performed inside the PVs. A contact force of seven grams was considered a minimum to deliver RF energy at any location. The power was adjusted to a range of 10–25 W when the ablation catheter was inside the CS, near a PV ostium or on the posterior LA wall. Point by point applications were performed (no dragging). At each RF application location, we sought for a complete “flattening” of the bipolar signal amplitude. The endpoint of ablation of areas of dispersion was AF termination defined as conversion to SR, or a stable atrial tachycardia (AT).(15) Post-ablation ATs were mapped and ablated until conversion to SR. If AF did not terminate after ablation of the pre-selected dispersion area regions, a new multi-electrode sequential map was performed (re-mapping). If two ablated

areas were very close (<1cm) they were connected by RF applications. Neither PV isolation nor linear ablation was performed.

After restoring SR by ablation, AF re-inducibility was tested by rapid atrial pacing (500–180 ms) in the proximal and distal CS with the addition of isoproterenol when the latter had been necessary to induce AF at the outset of the procedure. When ablation at dispersion regions led to rhythm regularization into AT before that all dispersion regions had been ablated, the AT was mapped and ablated. We mapped the AT in constructing activation maps and validating catheter location with the measurement of post-pacing intervals. After AT ablation, we performed pacing maneuvers in order to induce an arrhythmia, which manifested as either AF or AT. If AF was initiated, we completed the ablation set by applications at all dispersion regions that were not previously ablated. When AT was instead initiated, the AT was mapped and ablated. When AF or AT were no longer inducible but that some dispersion areas had not been ablated, we concluded the ablation with applications at dispersion regions that were not previously ablated (except for those areas within dispersion regions that were positioned in regards of the esophagus). In patients in whom SR was restored after more than two hours of procedure time, AF re-inducibility was not tested.

Ablation protocol in the validation set—For patients with paroxysmal AF, antral pulmonary vein isolation was performed. For patients with persistent AF, ablation using the stepwise approach(16) was performed (details in the online supplemental manuscript).

Dispersion regions location and surface area—In 90 patients, the location of dispersion regions — as tagged on the 3D bi-atrial electro-anatomical maps — was sorted according to a bi-atrial segmentation previously reported.(15) The total surface area occupied by dispersion regions and the surface area of the ablated regions were measured from the electro-anatomical maps in 43 patients. Biatrial surface was calculated with the CARTO software function after having excluded the areas pertaining to the mitral and tricuspid annuli, the vena cavas and the pulmonary veins.

Inter and intra-observer visual analysis variability of spatio-temporal dispersion—Fifty nine Pentaray EGMs in dispersion and non-dispersion regions were collected from five patients, mixed and blindly analyzed by four operators from the study. In order to assess the intra-observer variability, this analysis was repeated a few days later by the same operators but in a different order.

Time stability of the anatomic distribution of dispersion regions—We have examined the temporal stability of the spatial distribution of dispersion locations in the same patient. We have re-mapped patients after about 20 minutes and we compared the distribution of the dispersion region on 3D geometries of the atria. To also examine inter-observer stability of regions over time, the re-mapping was either performed by the same ablationist (n= 13 patients) or by a different ablationist (n= 7 patients).

Follow-up—All patients were instructed to contact the study center if they experienced palpitations or any other symptoms suggestive of recurrent AF and to discontinue antiarrhythmic drug therapy in the absence of symptoms after a 3-month blanking period.

They also had follow-up visits and 24-hour Holter monitors at 3, 6, 12, and 18 months of follow-up. In a subgroup of 20 patients, the rhythm was monitored with 7-day Holter monitors (n=18) or the memory functions of pacemakers and internal cardiac defibrillators (n=2). Patients with recurrent AF or AT—defined as arrhythmia episodes >30sec after the blanking period — were offered a second ablation procedure. For the redo procedures, the ablation protocol was similar to the one described above for the study group.

Study endpoints—The primary acute efficacy endpoint was AF termination. Secondary acute efficacy endpoints were conversion to SR and post-ablation AF non-inducibility. At the end of the 18-month follow-up period, our primary long-term efficacy endpoint was AF recurrence rate after a single procedure (with or without antiarrhythmic drug therapy). Secondary long-term efficacy endpoints included: AF/AT recurrence rate after one procedure (with or without antiarrhythmic drug therapy), AF/AT recurrence rate after and one or more procedures (with or without antiarrhythmic drug therapy), AF recurrence rate and AF/AT recurrence rate in the absence of antiarrhythmic drug therapy (*See details in the* supplemental material).

Mechanistic study

Mechanisms of post-ablation atrial tachycardias—We analyzed AT mechanisms and locations in a sub-set of 21 patients, in whom post-ablation tachycardias occurred during the index procedure or during the follow-up.

Automated mapping of fractionation—We sought to compare the surface area occupied by CFAEs, classically used as ablation targets, with the one of dispersion regions. We generated automatic fractionation maps (“auto-CFAEs”) with the CARTO setting “SCI 30–40”(17) : 30 and 40 ms as lower and upper limits, respectively. This setting is less sensitive to the detection of electrogram fractionation than the default setting (60–120 ms). In 40 regions (2 dispersion areas and 2 non-dispersed regions in 10 patients), we calculated the auto-CFAEs surface area/dispersion surface area ratio and the auto-CFAEs surface area/non-dispersion surface area ratio.

Quantification of spatio-temporal dispersion in numerical simulations and optical mapping experiments—In order to examine the mechanisms of spatio-temporal dispersion in AF driver regions, we analyzed intra-cardiac electrograms in dispersion and non-dispersion areas, which were the tagged and untagged regions, respectively. Also, we conducted numerical simulations and isolated ovine heart experiments to generate pseudo multipolar recordings in driver and bystander regions (see online supplemental manuscript). From simulations and optical time-series, we quantified spatio-temporal dispersion of electrogram fractionation. Each pseudo-bipolar electrograms from a virtual Pentarray was analyzed to determine its voltage absolute value (VAV) at each time point. Then the maximal VAV (VAVmax) among the 10 pseudo-bipoles of the virtual Pentarray was collected at each time point to form a new time-series VAVp. Finally, histograms of the distribution of VAVp values were presented in bins of 0.1 mV (MATLAB software, see Figures 7 and 8).

Statistical analysis—Categorical variables are expressed as n (%), and numerical variables as mean ± standard deviation or median [Quartile1–Quartile3]. Categorical variables were compared using the Chi-square test or Fisher exact test as appropriate. Continuous numerical data were compared using the Wilcoxon test or Brown-Mood median test as appropriate.

Survival analyses were performed to compare endpoints at the end of follow-up period: Kaplan Meier estimates for AF rates after a single procedure, AF/AT rates after a single procedure and AF/AT rates after one procedure or more (with or without antiarrhythmic drug therapy) (*See* supplemental material for details). Kaplan-Meier survival curves were assessed and compared using log-rank test. The time recorded was the time needed for the event of interest to occur (failure to achieve freedom from AF or freedom from AF and AT). The outcome is unknown in patients who did not reach the event before the end of follow-up (i.e. an 18-month follow-up), in patients lost to follow-up and in patients who died during the follow-up. In all such cases, the time of follow-up was recorded, and interpreted as censored data. Pairwise Cox hazards regression was used to compare survival of dispersion area subgroups (paroxysmal, persistent, and LS-persistent). A two-sided p-value<0.05 was used to indicate statistical significance. All statistical analyses were performed using SAS 9.1 software (SAS Institute Inc., Cary, NC).

Results

Clinical study

Patient characteristics—Between September 2013 and July 2014, 126 consecutive patients with AF were prospectively enrolled at three centers. Eighteen patients were excluded because of previous AF ablation and three patients because of the detection of a left appendage thrombus prior to ablation. In total, 105 patients were enrolled (Table 1).

Thirty two percent of patients were taking amiodarone at the time of the procedure. The mean LA volume was 168 ± 45 ml and 65 patients were in AF spontaneously at the beginning of the procedure (80% of the patients in non-paroxysmal AF). The validation set contained 47 patients. Comparisons between the study population and the validation set are shown in Table 1. Although patients in the validation set were younger (p=0.0046), the study population and the validation set were comparable in regards to AF type, AF duration, structural heart disease, hypertension, diabetes, LA diameter and baseline left ventricular ejection fraction.

Pre-ablation mapping—Before ablation the RAA and LAA reference CLs were 179[177–206] (184 ±33 ms) and 182[164–203] ms (186±35 ms), respectively. The mapping times and number of acquisition points/patient in the right and left atria were: 7[5–9] (7±3) and 12[10–15] (13±5) minutes, and 491[325–704] (512±325) and 882[673–1110] (927±436) points, respectively.

Figure 3A–C shows representative dispersion areas in three patients with paroxysmal, persistent and long-standing persistent AF. These maps illustrate that dispersion areas were formed by a variable number of electrograms (Figure 3A–C, white dots: clusters of

electrograms) and were patient- and AF form-dependent. The detailed characteristics of dispersion areas are presented in Table 2. There was an average of 5 ±1.5 dispersion areas/ patient. Each dispersion area spanned an average of 5 ± 2 cm^2. Dispersion areas covered a significantly larger surface area in patients with long-standing persistent AF than in patients with paroxysmal or persistent AF. Table 3 describes the locations of the dispersion areas.

Inter and intra-observer visual analysis variability of spatio-temporal dispersion: The visual analysis of the 4 operators was completely concordant in 94.3% of the analyzed EGMs (inter-observer variability equal to 6.7%). The intra-observer variability of the visual analysis was 2 ± 2% (5%, 1.7%, 1.7% and 0%. respectively for each operator).

Time stability of the anatomic distribution of dispersion regions: We observed a high degree of temporal stability in the spatial distribution of dispersion regions, regardless of whether the repeat mapping was performed by the same or a distinct ablationist. Precisely, when the two dispersion region maps were obtained by the same operator, the average dispersion region area was 30±12 cm^2 (~14% of the bi atrial surface) and 28 ±12 cm^2 (~13% of the bi atrial surface), n=13, for the first and second map, respectively. These two maps presented with a "matching" dispersion region area of 26±13 cm^2 (~12% of the bi atrial surface). If the two dispersion region maps were obtained by distinct operators, the average dispersion region area was 32±11 cm^2 (~11% of the bi atrial surface) and 29 ±8cm^2 (~10% of the bi atrial surface), n=7, for the first and second map, respectively. These two maps presented with a "matching" dispersion region area of 23±7 cm^2 (~8% of the bi atrial surface) (figure S6).

Ablation results

Procedural outcome (Figure 4, S2)—Ablation was performed in both the left and right atria in 51% of the patients. In the remainder of the patients, ablation was only performed in the left atrium. AF terminated in 100/105 patients (95%). In patients in "spontaneous" AF at the procedure outset (i.e in whom AF was not induced by pacing maneuvers, n=65) the AF termination was obtained in 60 patients (92%). In comparison, AF termination was obtained in all patients in whom AF was pace-induced (n=40,100%, p= 0.15). Off note, there were 25/65 patients (33.8%) with spontaneous AF on antiarrhythmic drugs vs 12/40 patients with induced-AF on antiarrhythmic drugs (30.0%): p=0.68. AF termination was obtained with 20 [10–37] (25.5±19.3) min of RF energy and 46 [21–72] (53±39.6) min after the 1st RF application either by conversion directly to SR (15%) or by conversion to AT (85%, Figure 4A). Overall, conversion to sinus rhythm was obtained by ablation in 77% of the patients.

Post-ablation AF inducibility was tested in 61 patients (58.6%). Non-inducibility of AF and AT was achieved in 72% of patients tested (44/61). An average of 1.93±1 ATs were ablated (Figure 4A). No major complications occurred. Three patients experienced minor groin bleeding. Radiofrequency time to terminate AF was significantly longer in longstanding persistent AF vs. both paroxysmal and persistent AF (p=0.0004, Figure 4B). The procedure time to terminate AF was significantly longer in long-standing persistent AF vs. paroxysmal AF (p=0.007, Figure 4B). For total procedure and RF times, there was no difference between AF types (Figure 4C).

In the validation set, the AF termination and SR conversion rates were significantly lower (Figure 4D). Also, the overall average procedure, radiofrequency energy, and fluoroscopy times were significantly longer in the control group: 230±67 minutes vs.168±42 minutes (p<.0001), 85±35 minutes vs. 49±21 minutes (p=0.0001), and 78±25 minutes vs. 15±13 minutes (p<.0001) respectively (Figure 4E and Table S1). RF energy times for paroxysmal AF ablation were similar between the study population and the validation set (Table S1).

Finally, we did not check whether PVs were isolated. Therefore, we cannot state that some of the PVs were not unintentionally isolated. In 13 additional patients, in whom we only performed dispersion ablation, 52 PVs were assessed for electrical isolation. Two out of 52 PVs were isolated unintentionally.

Ablated area—The area that was ablated represented 10 ± 5% of the overall bi-atrial area and 17 ± 10% of the LA area. Notably, the areas ablated in paroxysmal and persistent AF patients were comparable, but the area ablated in patients with long-standing persistent AF was significantly larger (see Table 2).

Long-Term results—Ninety six patients (91.4%) in the study population completed the 18-month follow-up. Nine patients (8.6%) did not complete the 18-month follow-up: one patient died two months before the end of the follow-up (myocardial infarction) and eight patients were lost to follow-up because of relocation. Their mean follow-up time was 10±3 months. In the validation set, three patients dropped out during the blanking period (one patient died because of heart failure and two relocated). All the other patients completed the 18-month follow-up.

The single-procedural AF recurrence rate outcome and the single procedural AF/AT recurrence rate outcome after 18 months of follow-up was significantly lower in the study population compared with the validation set: 11% vs 58%, log rank *P<0.001* and 45% vs 64%, log rank *P=0.026* (AF free-survival rates = 89% vs 42%, log rank *P<0.001* and AF/AT free-survival rates = 55% vs 36%, log rank *P=0.026*) (figure 5A). The multiple-procedural arrhythmia-recurrence rates were also lower in the study population at the end of the follow-up: 15% vs 41%, log rank *P<0.001* (AF/AT free-survival rates =85% vs 59%, log rank *P<0.001*) (figure 5B and figures S4–5 showing data from 7-days Holter monitors). Importantly, there was a comparable rate of patients under anti-arrhythmic drugs in the study group vs. in the validation set: 44% vs. 43%, respectively, p=0.9.

After one procedure, there were no differences in AF recurrence or AF/AT recurrence rates between the paroxysmal, persistent and long-standing persistent groups: respectively 21%, 8%, 10%, log rang *P*=0.24 and 29%, 53%, 43%, log rank *P* =0.15 (AF free-survival and AF/AT free-survival rates : respectively 79%, 92%, 90%, log rang *P*=0.24 and 71%, 47%, 57%, log rank *P* =0.15). After 1.4±0.5 procedure/patient there were no differences in AF/AT recurrence rates between the paroxysmal, persistent and long-standing persistent groups respectively: 17%, 16% and 13%, log rank *P=0.9* (AF/AT free-survival rates: 83%, 84% and 87% respectively, log rank *P=0.9*). Re-do procedures were performed for organized ATs in 75.6% of the patients. Re-dos were significantly shorter in duration than the index

procedures and required less RF and fluoroscopy times (Table S2). Except for one pericardial effusion, no major complications were noted after the re-do procedures.

We then compared key patient and procedure characteristics between patients who were "spontaneously" in AF at the beginning of the procedure (no pacing maneuver) vs. the ones of patients in whom AF had been pace-induced. For pace-induced and "spontaneous" AF patients respectively, the LA volumes were 143±31 vs. 181 ±46, p< 0.0001; the RF times to terminate AF 19.8 ±16.2 vs. 29.4 ±20.4 min., p=0.02; the total RF times 43 ±19.7 vs. 52.3 ±21.5 min., p=0.01; the rates of AF termination were 100 and 92% (p=0.15). However, after an 18-month follow-up and an average of 1.4 procedures in both sub-groups, there was a similar rate of AF/AT recurrence between "spontaneous" AF and paced-induced AF (14% vs. 18% respectively, log rank *P=0.44*). We observed no statistical difference in outcomes at the end of the follow-up between patients on and off anti-arrhythmic medications: the AF recurrence rate after a single procedure was 13% for those on drugs vs 10% for those off drugs, log rank *P* =0.62; the AF/AT recurrence rates after a single procedure were 46% for those on drugs vs 44% for those off drugs, log rank *P* =0.71 and the AF/AT recurrence rates after one procedure or more was 15% in patients on or off drugs, log rank *P=1.00.*

Mechanistic study

Mechanisms of post-ablation atrial tachycardias

(i) ATs during the index procedure: In 21 patients, we counted 44 distinct ATs (2.2±1.3 AT/patient): 22 were macro reentries (peri-tricuspid, perimitral or LA roof flutters) and 22 were localized AT (focal or micro-reentries). Of these 44 ATs, only 5/44 (11.4%) originated from dispersion regions that had just been ablated while 39/44 (88.6%) were either macro-reentries or localized ATs arising from locations which were not previously ablated. Importantly 17/22 localized ATs arose from dispersion regions that were not previously ablated (figure S7).

(ii) ATs that occurred during the follow-up (re-do procedures): We analyzed the long-term AT recurrences after the index AF ablation procedure. We focused our analysis on determining whether the AT that occurred arose from the dispersion regions that were targeted during the index procedure (dispersion-index regions) or from non-dispersion regions (non-dispersion-index regions), which were not ablated. During the follow-up period, eleven AT ablation procedures were conducted. In total, 18 distinct recurrent ATs were analyzed.

- 11/18 ATs (61%) originated from non-dispersion-index regions as follows: six macro-reentries previously ablated at non-dispersion regions such as the mitral isthmus or the roof relapsed presumably because of conduction recovery of ablation lines; four macro-reentries which were not present during the index case. Finally, one focal tachycardia arose from a non-dispersion-index region.
- 3/18 (16.6%) ATs originated from within a dispersion-index region.
- 4/18 (22%) were found in close vicinity of a dispersion-index-region (<1 cm).

Automatic Detection of fractionated signals—The ratios of surface area of CFAEs detected by the CARTO software to the surface area of dispersion regions, and of the surface area of CFAEs detected by the CARTO software to the surface area of regions that did not display dispersion were 72+/−25 % and 27+/−15% respectively (figure 6A and online supplemental Figure S3).

Off-line multipolar electrograms analysis—Dispersion area abnormal electrograms exhibited a higher occurrence of single-bipole fractionated continuous signals (Figure 6B), a reduced voltage (Figure 6C), a significantly shorter cycle length (Figure 6D), and that dispersion duration spanned most of the AFCL (Figure 6E–F). In addition, Figure 6G demonstrates that a mean of 8.1±3.5 rotations per 2.5 seconds occurred in dispersion areas.

Numerical simulations and optical mapping experiments

(i) Fast rotational vs. slow non-rotational simulated multipolar electrograms: Figure 7 depicts simulated pseudo-multipolar electrograms obtained after positioning a virtual PentaRay either at the center or at the periphery of driver (here a rotor, Figure 7A–C and Supplemental Online Movie 1). In comparing Figure 7A and 7B, striking differences in the features of the virtual PentaRay electrograms may be seen. When the virtual catheter hovers over the center of the driver, virtual bipolar electrograms exhibit a fast frequency of excitation. Also, the time distribution of the electrograms is such that either branch of the PentaRay is activated in asynchrony with the other branches. As a result, the virtual electrograms time-series span most of the AFCL. The overall visual impression is one of successive electrode-to-electrode and branch-to-branch activations. At the periphery of the driver, the frequency of activation is reduced and impulses are non-rotational or planar-like. As a result, either branch of the PentaRay is activated in relative synchrony with the other branches (Figure 7B). The visual impression is one of successive beats separated by quiescence.

(ii) Role of interstitial fibrosis: In Figure 7C, we show an AF driver initiated in a pseudo-fibrotic substrate. In this setting, driver impulses propagate within a highly heterogeneous substrate. As a result, the virtual PentaRay generates unique multipolar pseudo-electrogram features. Throughout the 2D sheet, multiple regions contribute to a slowing down of the rotational impulse. Although there is no impulse block, the driver's wavefront experiences markedly slow and heterogeneous conduction. This results in beat-to-beat changes in wave directionality. Such disturbances translate into lengthened depolarization pseudo-electrograms (Figure 7C), reminiscent of the features of dispersion areas in patients. Here, the numerical and experimental data predict that such drivers should yield electrograms with significantly greater temporal and spatial dispersion than drivers spinning within relatively homogeneous media.

Optical mapping—Figure 8 A–B presents pseudo-multipolar electrograms generated from optical movies during AF induced in an isolated left-atrial-scar heart (see online supplemental methods). The PentaRay-like single-pixel time series were obtained in the region of the LAMI border zone where a driver was anchored after initiation by burst pacing (see Online Supplemental Movie 2). For comparison, we present PentaRay-like single-pixel

time series obtained at the RA where non-rotational and planar-like waves propagated (see online supplemental movie 2). Similarly to the differences seen in the simulations, fractionated multipolar pseudo-electrograms exhibit a high degree of spatio-temporal dispersion when they are recorded in in the vicinity of a driver (Figure 8B, right panel). In the RA bystander region, however, waves are planar-like and pseudo-electrograms are nearly simultaneous (Figure 8B, left panel). These aspects evoke the dispersion areas and non-tagged multipolar electrograms aspects recorded in patients. In addition, the VAVp times series shown in the right panels of Figures 7 and 8 illustrate that the time of electrical quiescence of pseudo-multipolar electrograms obtained in the vicinity of a driver, — i.e low <0.2 mV VAVp values — is drastically reduced in comparison with the time of electrical quiescence of pseudo-multipolar electrograms from bystander regions. Collectively, our simulations and optical mapping studies suggest that dispersion areas may be regarded as electrogram footprints of active electrical sources of AF propagating in a heterogeneous atrial muscle.

Discussion

Our main findings are as follows:

- **i.** Spatio-temporal dispersion of electrograms represents an electrical footprint of waves emanating from rapid fibrillatory drivers and propagating within a heterogeneous atrial muscle.
- **ii.** The clustering of intra-cardiac electrograms exhibiting spatio-temporal dispersion may guide a wholly patient-tailored ablation of all types of AF.

A Multipolar Electrogram-guided Approach to AF Ablation

The results of this pilot study demonstrate that electrogram dispersion detected by direct visualization of electrograms recorded simultaneously with a splined, multi-electrode catheter is a marker of AF drivers. We recorded regions exhibiting spatio-temporal electrogram dispersion and targeted such regions in the absence of PV isolation or any other anatomy-based ablation. With 44% of patients on antiarrhythmic medication, our preliminary results show that our approach allowed for efficacious, non-extensive and patient-tailored ablation of all types of AF. Twenty minutes of RF energy application resulted in a 95% rate of AF termination and 89% of patients were free from AF after a single procedure and 18 months of follow-up. The AF/AT free-survival rate was 55% after one procedure and 85% after ~1.4 procedures/patient.

This study offers insight into why CFAEs may represent worthy ablation targets in some hands,(6–8) but not in others.(1–5) Successful outcomes after ablating CFAEs may be explained by the fact that fractionated electrograms represent a majority of the surface area in driver regions (Figure 6A), which exhibit spatial and temporal dispersion. On the other hand, fractionated electrograms may also be found in bystander regions that do not exhibit dispersion (see Figure 2C, 6A and online supplemental Figure S3). We indeed show that CFAEs located in non-dispersion regions represent the majority of the CFAEs surface area. Besides, there is about 30% of the surface area in dispersion regions that are sites of non-fractionated electrograms (see Figure 6A). Altogether, we present evidence which supports

that dispersion ablation may overlap with conventional CFAEs ablation when CFAEs are spatially clustered. Also, our numerical and experimental data strongly suggest that dispersion regions corresponds to driver regions, which may be identified either on the endocardial or epicardial sides of the atrial wall. Future works implementing advanced mapping simultaneously to multipolar electrode recordings are needed to examine the degree of overlap between driver and dispersion regions.

Also, the current contribution jives well with the Narayan et al. and Jadidi et al. contributions.(14,18) in that they suggest that patient-tailored, mechanism-based ablation may yield valuable results. We envision such studies as well as our study as the building blocks of a collaborative effort, which may lead to an efficacious patient-tailored ablation approach. In the Narayan et al. study the ablation time for reaching the acute endpoint of AF termination or ≤ 10% AF slowing was 31.8 (22.1–71.5) and 18.5 (7.9–24.5) min in the FIRM-blinded and the FIRM groups, respectively.(14) After having performed PVI, ablation times increased to a total of 52.1 ± 17.8 and 57.8 ± 22.8 min., respectively. In the Jadidi et al. study, the PVI was the initial ablation approach. PVI was achieved after a mean of 28±11 minutes. In those patients in whom PVI did not terminate AF, selective atrial ablation at low-voltage, dispersion-like regions terminated persistent AF after 11±9 minutes (range: 1–18 minutes) of RF. Then, ablation of the remaining ATs required an additional 12±9 minutes resulting in a total RF time of 23±11 minutes in addition to PVI, with a grand total of 44±19 minutes of RF.(18) The main difference, however, with the present work is the percentage of the overall ablation time that was dedicated to patient-tailored ablation. This represented about one third of the overall ablation in the Narayan et al. contribution, half in the Jadidi et al. study and all the ablation in our study. *Therefore, we feel that the most novel aspects of our approach is that it represents an approach that is entirely patient-tailored.*

The comparison with a validation set provides further evidence that dispersion ablation was comparable to a more conventional ablation approach (Figures 4 and 5 and Table S1). Finally, after dispersion ablation the majority (75.6%) of the recurrences were organized AT — and not AF. ATs were simpler to ablate as demonstrated by the reduction in procedure time and the higher SR conversion rate during re-do ablation (see Table 4). We believe that such a high proportion of AT recurrences/AF recurrences may be the basis for our highly satisfactory long term outcomes: 85% of patients free from any arrhythmia after ~ 1.4 procedures/patient in a population with 77% of persistent and long-standing AF.

Electrophysiological Mechanisms underlying Multipolar Electrogram Dispersion

Here we have conducted numerical simulations and experiments to examine the mechanisms by which regions harboring spatio-temporal dispersion of electrograms are key to AF perpetuation. Both our experiments and numerical simulations show that pseudo-multipolar electrograms exhibiting dispersion are uniquely recorded in the vicinity of drivers (see Figures 7 and 8). Such results illustrate that the simultaneous presence of time and spatial dispersion of abnormal electrograms represents regions where the wavefront shape is highly curved and where impulse propagation of waves emanating from drivers is impaired. This also corroborates previous findings that continuously fractionated electrograms, which could be seen as dispersed electrograms, have been recorded in rotor regions,(15) or in regions

critical to AF maintenance. Importantly, our results demonstrate that the dispersion of multipolar electrograms is highly dependent on both the source's frequency of activation and its underlying atrial substrate (see Figures 7 and 8). We previously reported that beat-to-beat changes in wavefront directionality and impulse velocity produce fractionation in the immediate vicinity of a rotor at the boundary of the maximal dominant frequency domain.(19) This was expected as several studies had emphasized that electrogram fractionation is highly frequency-dependent. (11,19–21) In particular Spach et al. presented that electrogram fractionation that occurs during transversal impulse propagation may also manifest in the longitudinal direction at shorter cycle lengths (frequency-dependent space dispersion).(20) Here, our results corroborate these findings in showing that spatio-temporal dispersion of multipolar electrograms is frequency-dependent. Therefore, our results also validate the studies that indicated that high dominant frequency may be used as a surrogate for the localization of AF sources.(22–24).

The fact that post-ablation ATs predominantly arise from non-ablated dispersion regions suggests the unmasking of AT drivers after some degree of substrate modification. While this is a plausible scenario, it is unclear how ablation may prevent fibrillatory conduction of waves emanating from the (subsequent) AT drivers while, at the same time, reducing the overall frequency of activation. This would suggest that a single ablation application could produce effect on an AT driver as well as on distant waves emanating from it. An alternative scenario may be that post-ablation ATs arising from non-ablated dispersion regions pre-exist but as secondary, or co-primary drivers. Once the first driver(s) has(ve) been ablated the arrhythmic activity may only be maintained by slower drivers. These may only rise to dominance once their faster counterpart, located in a distinct dispersion region, has been ablated.

Besides, we demonstrate that interstitial fibrosis is key to the observation of spatio-temporal dispersion of electrograms during AF. Previously, we and others had reported that fractionated electrograms may be recorded in regards of rotors propagating within a fibrotic atrium.(24,25) Here, we show that a driver initiated whithin a fibrotic atrium (Figure 7C) yields a significantly larger temporal and spatial electrogram dispersion than the one produced by a driver propagating within a more homogeneous medium (Figure 7B). As we have previously shown,(24) the presence of fibrotic, millimeter-sized obstacles (1–7 mm2) is sufficient to anchor reentries characterized by a cycle length that depends on the obstacle size. Therefore, in the context of extensive fibrosis, the term rotor, which may be understood as an "entirely functional" reentry, may be inter-changeable with terms such as micro-reentry or reentry that also are AF drivers. Overall, these results agree with recent atrial structural imaging reports, which have presented that the atria of patients undergoing AF is highly fibrotic, and that electrograms fractionation occurs in regions of patchy fibrosis.(26–28)

Limitations

The non-randomized design of this pilot study limits our conclusions in comparing techniques. An evaluation of dispersion area ablation in a larger patient population using a randomized study design is warranted. Also, in patients in SR at the outset of the procedure

and in whom AF is initiated by pacing maneuvers, the assumption should be that RF ablation may lead to a serendipitous termination. The results presented herein indicate that paced-induced AF patients are somewhat “easier” to ablate as previously reported by Haissaguerre et al.(15) Still, their long-term AF/AT free-survival rate is similar to the one of spontaneous AF patients. Here, however, the long-term AF/AT free-survival rate between “spontaneous” and paced-induced AF patients was similar (86% vs. 82%, respectively, log rank *P=0.44*). In general, procedural endpoints such as AF termination, SR conversion or AF non-inducibility need to be interpreted with caution. Besides, their value as procedural predictors of long-term outcome will need to be rigorously investigated. Also, we did not assess whether PVs were isolated after dispersion ablation. Therefore, we cannot state that PVs were not unintentionally isolated. As indicated in the results section, preliminary results in additional 13 patients indicate that unintentional PV isolation after dispersion ablation is a marginal phenomenon (2/52 PVs). The computer simulations were performed in a 2D model. A more realistic 3D model of AF and fibrosis would yield more realistic electrograms. Finally, in order to avoid prolonged procedures and comply with institutional requirements, we made the collegial decision to withhold inducibility maneuvers after two hours.

Conclusions

We present the first demonstration that the clustering of intra-cardiac electrograms exhibiting spatio-temporal dispersion allows for a wholly patient-tailored ablation of all types of AF.

Supplementary Material

Refer to Web version on PubMed Central for supplementary material.

Acknowledgments

The authors thank their colleagues for their scientific input, in particular Drs. Fred Morady, Hakan Oral, José Jalife, Alexandre Maluski, Eloi Marijon and Julien Mancini. The authors also thank Fanny Desmettre, Julia Legrand, Alexandrine Lozupone, Camille Metzdorff, Joseph Ajoury, Alexandre Masse and Kamila Djouadi for their technical assistance. Special thanks to Donovan C. Jr for his drawings and his support.

Source of Funding

The study was not funded by industry and received no financial support. Dr Masatoshi Yamazaki was supported by Grant-in-Aid for Scientific Research (C): 15K09077 and Joint International Research: 15KK0341.

Abbreviation list

AF	Atrial fibrillation
AT	Atrial achycardia
CFAE	Complex fractionated atrial electrogram
CS	Coronary sinus
CL	Cycle Lengths

EGM	Electrogram
LAA	LA appendage
LA	Left Atrium
PV	Pulmonary vein
SR	Sinus rhythm
SD	Standard deviation
VAV	voltage absolute value

References

1. Verma A, Jiang C, Betts TR, et al. Approaches to catheter ablation for persistent atrial fibrillation. N Engl J Med. 2015; 372:1812–1822. [PubMed: 25946280]
2. Wong KCK, Paisey JR, Sopher M, et al. No Benefit OF Complex Fractionated Atrial Electrogram (CFAE) Ablation in Addition to Circumferential Pulmonary Vein Ablation and Linear Ablation: BOCA Study. Circ Arrhythm Electrophysiol. 2015 CIRCEP.114.002504.
3. Oral H, Chugh A, Good E, et al. Radiofrequency catheter ablation of chronic atrial fibrillation guided by complex electrograms. Circulation. 2007; 115:2606–2612. [PubMed: 17502567]
4. Providência R, Lambiase PD, Srinivasan N, et al. Is There Still a Role for Complex Fractionated Atrial Electrogram Ablation in Addition to Pulmonary Vein Isolation in Patients With Paroxysmal and Persistent Atrial Fibrillation?: Meta-Analysis of 1415 Patients. Circ Arrhythm Electrophysiol. 2015; 8:1017–1029. [PubMed: 26082515]
5. Vogler J, Willems S, Sultan A, et al. Pulmonary Vein Isolation Versus Defragmentation: The CHASE-AF Clinical Trial. J Am Coll Cardiol. 2015; 66:2743–2752. [PubMed: 26700836]
6. Nademanee K, McKenzie J, Kosar E, et al. A new approach for catheter ablation of atrial fibrillation: mapping of the electrophysiologic substrate. J Am Coll Cardiol. 2004; 43:2044–2053. [PubMed: 15172410]
7. Seitz J, Horvilleur J, Curel L, et al. Active or Passive Pulmonary Vein in Atrial Fibrillation: Is Pulmonary Vein Isolation always essential? Heart Rhythm Off J Heart Rhythm Soc. 2014
8. Seitz, J., Bars, C., Ferracci, A., et al. Electrogram Fractionation-Guided Ablation in the Left Atrium Decreases the Frequency of Activation in the Pulmonary Veins and Leads to Atrial Fibrillation Termination. JACC Clin Electrophysiol. 2016. [E-pub ahead of print]; http://linkinghub.elsevier.com/retrieve/pii/S2405500X16301050
9. Jaïs P, Haïssaguerre M, Shah DC, Chouairi S, Clémenty J. Regional disparities of endocardial atrial activation in paroxysmal atrial fibrillation. Pacing Clin Electrophysiol PACE. 1996; 19:1998–2003. [PubMed: 8945085]
10. Rostock T, Rotter M, Sanders P, et al. High-density activation mapping of fractionated electrograms in the atria of patients with paroxysmal atrial fibrillation. Heart Rhythm Off J Heart Rhythm Soc. 2006; 3:27–34.
11. Narayan SM, Wright M, Derval N, et al. Classifying fractionated electrograms in human atrial fibrillation using monophasic action potentials and activation mapping: evidence for localized drivers, rate acceleration, and nonlocal signal etiologies. Heart Rhythm Off J Heart Rhythm Soc. 2011; 8:244–253.
12. Ganesan P, Cherry EM, Pertsov AM, Ghoraani B. Characterization of Electrograms from Multipolar Diagnostic Catheters during Atrial Fibrillation. BioMed Res Int. 2015; 2015:272954. [PubMed: 26581316]
13. Haïssaguerre M, Hocini M, Sanders P, et al. Localized sources maintaining atrial fibrillation organized by prior ablation. Circulation. 2006; 113:616–625. [PubMed: 16461833]

14. Narayan SM, Krummen DE, Shivkumar K, Clopton P, Rappel W-J, Miller JM. Treatment of atrial fibrillation by the ablation of localized sources: CONFIRM (Conventional Ablation for Atrial Fibrillation With or Without Focal Impulse and Rotor Modulation) trial. J Am Coll Cardiol. 2012; 60:628–636. [PubMed: 22818076]
15. Haissaguerre M, Hocini M, Denis A, et al. Driver domains in persistent atrial fibrillation. Circulation. 2014; 130:530–538. [PubMed: 25028391]
16. Scherr D, Khairy P, Miyazaki S, et al. Five-year outcome of catheter ablation of persistent atrial fibrillation using termination of atrial fibrillation as a procedural endpoint. Circ Arrhythm Electrophysiol. 2015; 8:18–24. [PubMed: 25528745]
17. Seitz J, Horvilleur J, Lacotte J, et al. Automated Detection of Complex Fractionated Atrial Electrograms in Substrate-Based Atrial Fibrillation Ablation: Better Discrimination with a New Setting of CARTO® Algorithm. Jounal Atr Fibrillation. 2013:16–21.
18. Jadidi AS, Lehrmann H, Keyl C, et al. Ablation of Persistent Atrial Fibrillation Targeting Low-Voltage Areas With Selective Activation Characteristics. Circ Arrhythm Electrophysiol. 2016; 9:e002962. [PubMed: 26966286]
19. Kalifa J, Tanaka K, Zaitsev AV, et al. Mechanisms of wave fractionation at boundaries of high-frequency excitation in the posterior left atrium of the isolated sheep heart during atrial fibrillation. Circulation. 2006; 113:626–633. [PubMed: 16461834]
20. Spach MS, Dolber PC, Heidlage JF. Influence of the passive anisotropic properties on directional differences in propagation following modification of the sodium conductance in human atrial muscle. A model of reentry based on anisotropic discontinuous propagation. Circ Res. 1988; 62:811–832. [PubMed: 2450697]
21. Atienza F, Calvo D, Almendral J, et al. Mechanisms of fractionated electrograms formation in the posterior left atrium during paroxysmal atrial fibrillation in humans. J Am Coll Cardiol. 2011; 57:1081–1092. [PubMed: 21349400]
22. Sanders P, Berenfeld O, Hocini M, et al. Spectral analysis identifies sites of high-frequency activity maintaining atrial fibrillation in humans. Circulation. 2005; 112:789–797. [PubMed: 16061740]
23. Atienza F, Almendral J, Jalife J, et al. Real-time dominant frequency mapping and ablation of dominant frequency sites in atrial fibrillation with left-to-right frequency gradients predicts long-term maintenance of sinus rhythm. Heart Rhythm Off J Heart Rhythm Soc. 2009; 6:33–40.
24. Tanaka K, Zlochiver S, Vikstrom KL, et al. Spatial distribution of fibrosis governs fibrillation wave dynamics in the posterior left atrium during heart failure. Circ Res. 2007; 101:839–847. [PubMed: 17704207]
25. Ashihara T, Haraguchi R, Nakazawa K, et al. The role of fibroblasts in complex fractionated electrograms during persistent/permanent atrial fibrillation: implications for electrogram-based catheter ablation. Circ Res. 2012; 110:275–284. [PubMed: 22179057]
26. Jadidi AS, Cochet H, Shah AJ, et al. Inverse relationship between fractionated electrograms and atrial fibrosis in persistent atrial fibrillation: combined magnetic resonance imaging and high-density mapping. J Am Coll Cardiol. 2013; 62:802–812. [PubMed: 23727084]
27. Akoum N, Wilber D, Hindricks G, et al. MRI Assessment of Ablation-Induced Scarring in Atrial Fibrillation: Analysis from the DECAAF Study. J Cardiovasc Electrophysiol. 2015; 26:473–480. [PubMed: 25727106]
28. Akoum N, Daccarett M, McGann C, et al. Atrial fibrosis helps select the appropriate patient and strategy in catheter ablation of atrial fibrillation: a DE-MRI guided approach. J Cardiovasc Electrophysiol. 2011; 22:16–22. [PubMed: 20807271]

Perspectives

Competency in Medical Knowledge

This study demonstrates that the spatio-temporal dispersion of electrograms during catheter ablation is a multipolar electrogram signature of electrical drivers of atrial fibrillation.

Competency in Patient Care

A multiple-location dodecapolar electrode mapping serves in identifying small driver regions in the left and right atria. Ablation at such locations leads to AF termination in most patients.

Translational Outlook 1

Atrial regions exhibiting spatio-temporal dispersion are driving the fibrillatory activity. Numerical simulation and optical mapping experiments confirm that spatio-temporal dispersion of electrograms is the electrical signature of underlying drivers.

Translational Outlook 2

Automated software measurement of electrogram fractionation gives a highly inaccurate account of spatio-temporal dispersion of electrograms.

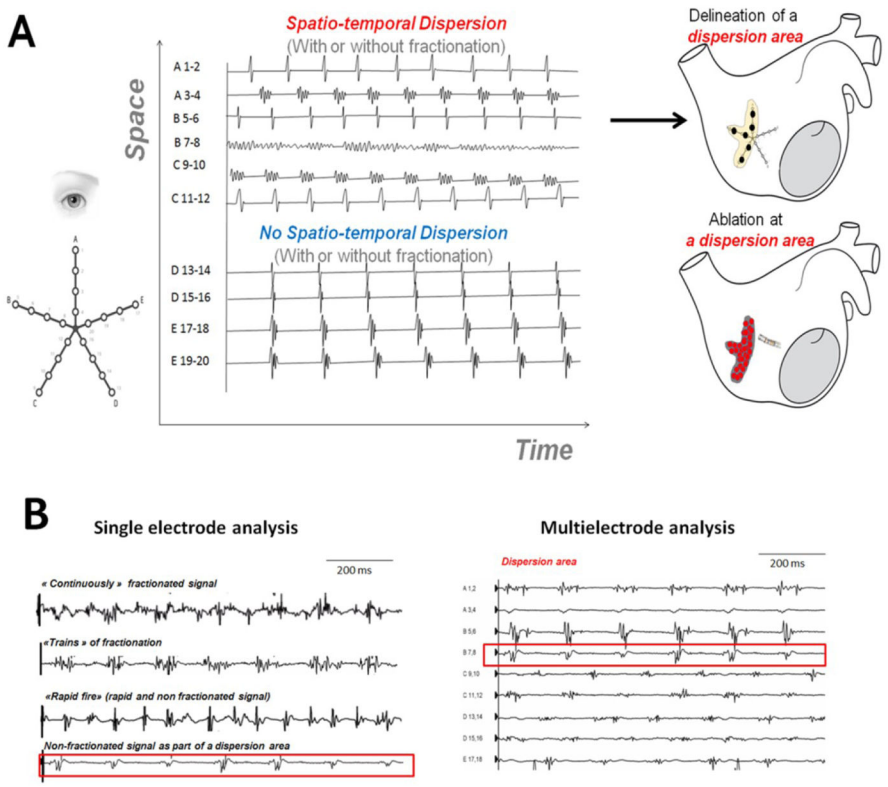

Figure 1. Spatio-temporal Dispersion of Multipolar Electrograms

Panel A: *Dispersion areas*: definition, mapping approach and delineation.

Panel B, Left: Examples of single-bipole signals from dispersion regions. **Upper:** Continuously fractionated and low-voltage signals. **Upper Middle:** "Trains of Fractionation" are periodic fractionated electrograms. **Lower Middle:** "Rapid Fires" are short-cycle-length non-fractionated electrograms. **Lower:** Non-fractionated (>120 ms) electrograms may be one or several of the electrograms within a dispersion region (**Panel B, right**). Collectively, the bipolar electrograms span most of the AFCL recorded in the region.

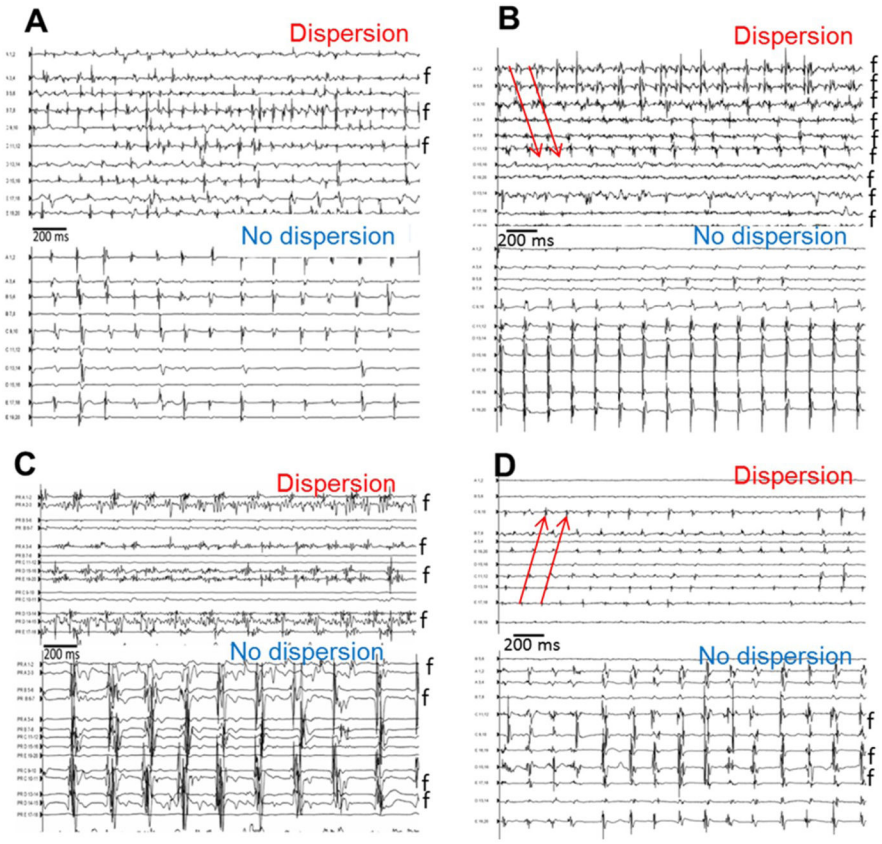

Figure 2. Examples of Spatio-temporal Dispersion

panels A–D: *Representative examples* of the multipolar electrograms (clusters of electrograms) recorded in dispersion and in non-dispersion regions in four patients. Fractionated electrograms are marked by an “f”. In the dispersion regions, it was common to find bipoles exhibiting continuously fractionated signal as shown in panels B and C. Red arrows show the sequential activation of consecutive bipoles of multielectrode catheter spanning 100% of the AF cycle length.

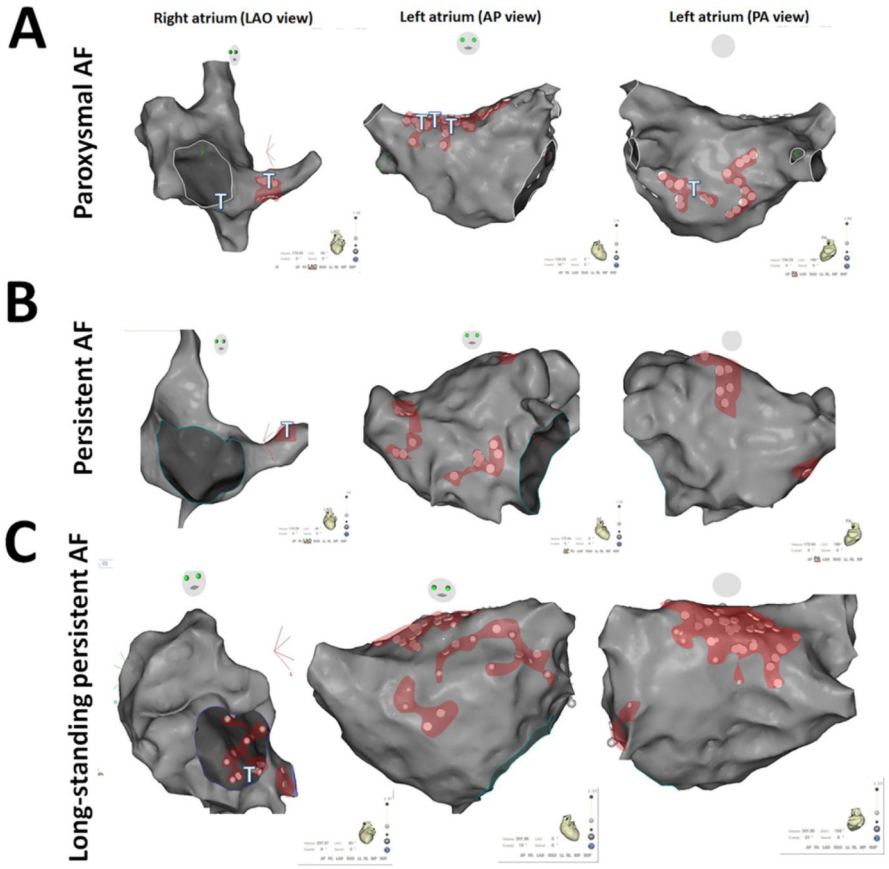

Figure 3. Examples of Dispersion Maps

Panels A, B, C: ***Dispersion regions delineated by clusters of electrograms*** (white dots)***: localization and extent***. CARTO renderings of dispersion regions in representative patients with paroxysmal (panel A), persistent (panel B) and long-standing persistent (panel C) AF. Left: left anterior oblique (LAO) view; middle: antero-posterior (AP) view; right: postero-anterior (PA,) view. Dispersion regions are shaded in red. Sites at which point ablation led to AF termination are depicted with a **T**.

(AP): antero-posterior

(LAO): left anterior oblique

(PA): postero-anterior

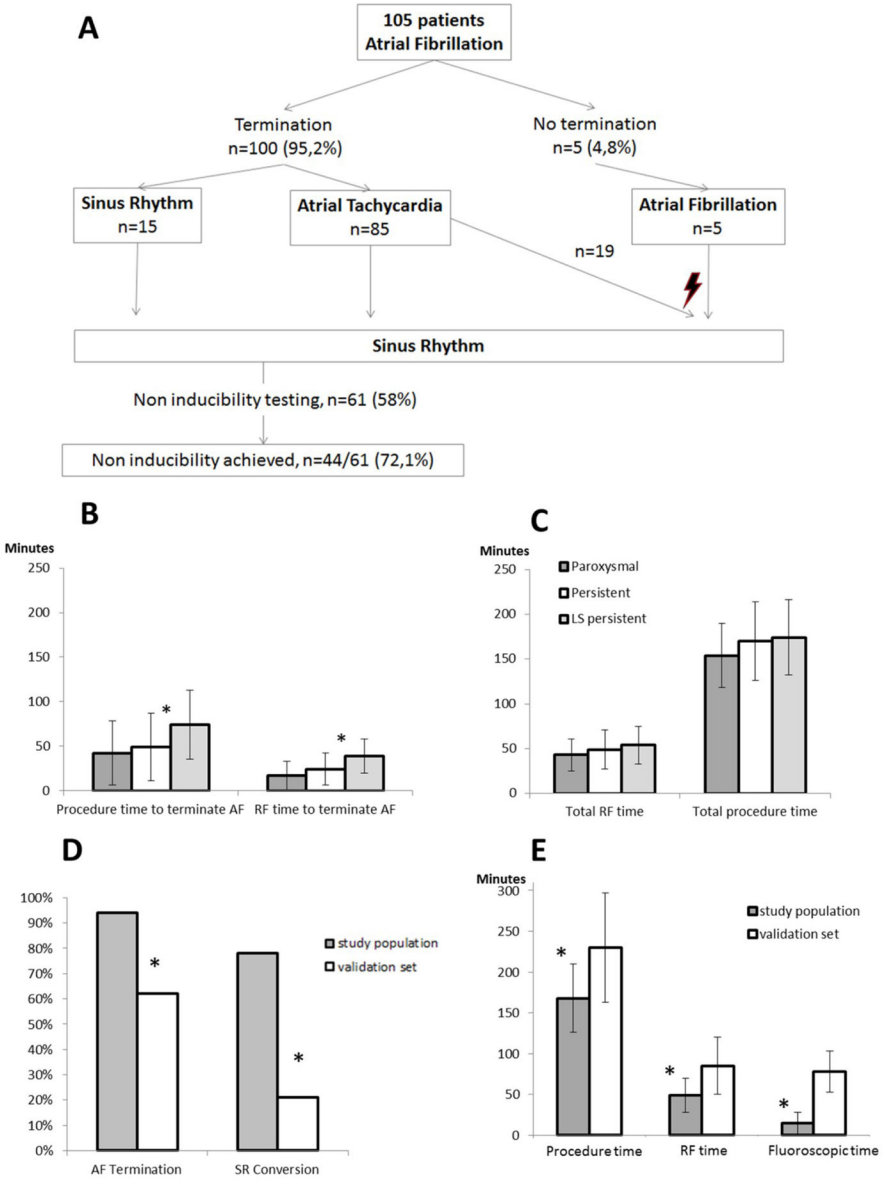

Figure 4. Procedural Outcomes

Panel A: Flow-chart depicting the per-procedural outcome.

Panel B: Procedure (left) and radiofrequency (right, RF) time to terminate AF. *: p<0.01.

Panel C: Procedure (left) and radiofrequency (right, RF) time. P>0.05 between all AF types.

Panel D: AF termination and sinus rhythm (SR) conversion by ablation in the study population compared to the validation set (left, persistent and long-standing persistent lumped together). *: p<0.01.

Panel E: Procedure, radiofrequency (RF) and fluoroscopic times in the study in the study population compared to the validation set. *: p<0.01.

(RF): radiofrequency

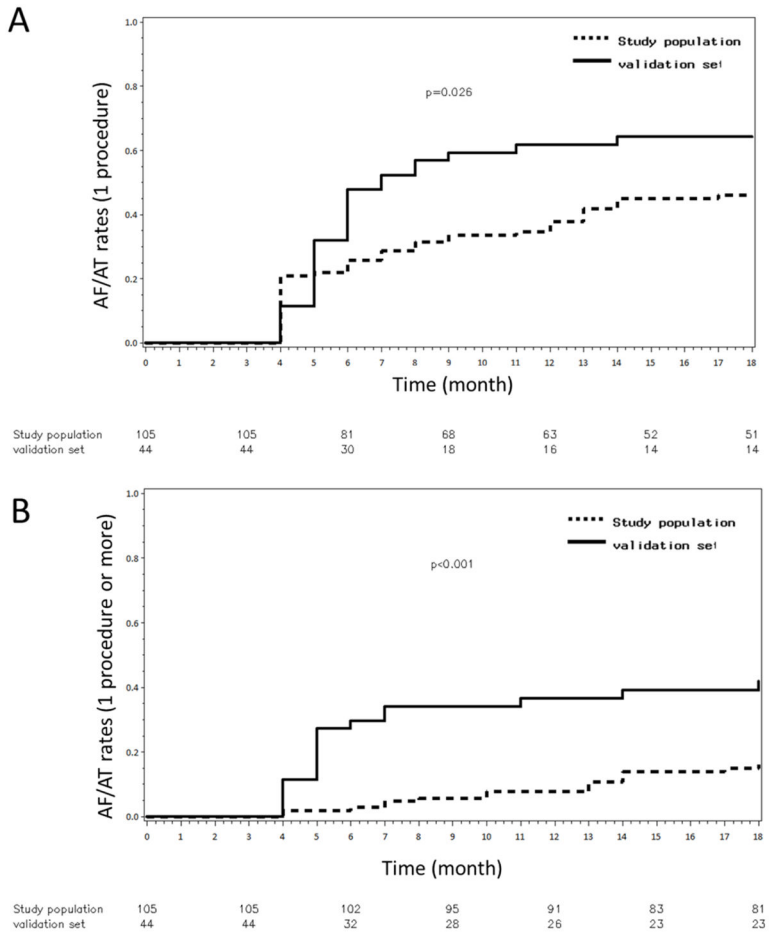

Figure 5. Eighteen-month Outcome

Panels A–B: Kaplan-Meier curves illustrating AF/AT recurrence rates after a single procedure (**A**) and after multiple procedures (**B**) in the study population and the validation set.

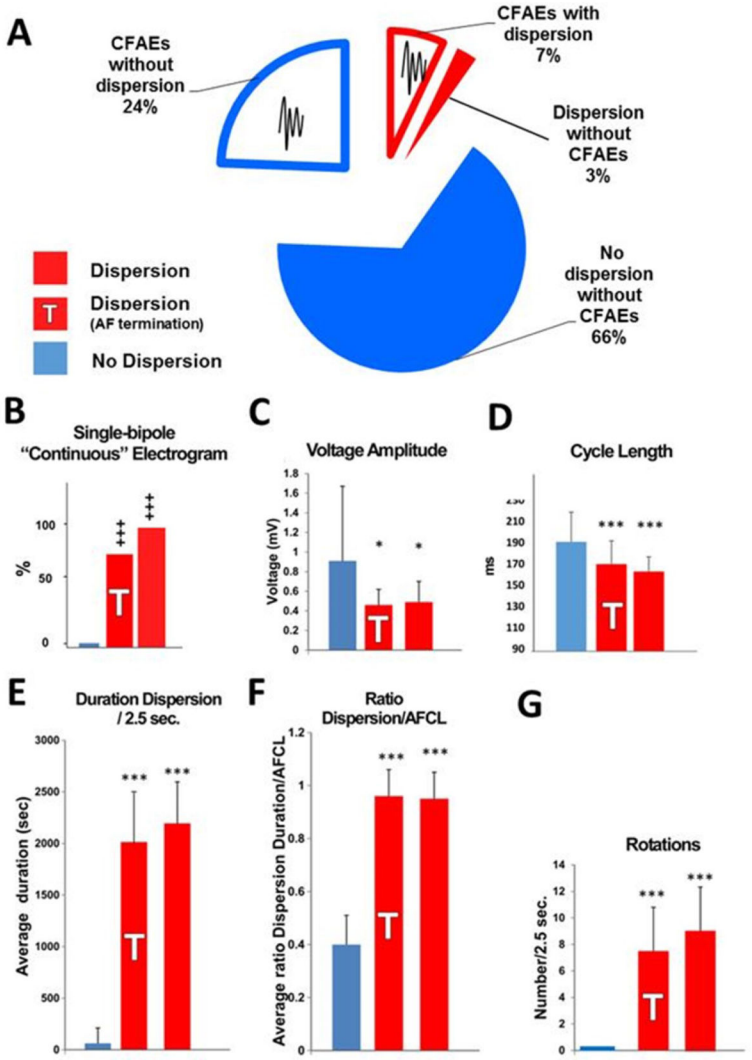

Figure 6. Signal Analysis

Panel A: Pie chart of the surface area of fractionated electrograms tagged with the CARTO algorithm (auto-CFAEs) in dispersion (red) and non-dispersion (blue) regions. CFAEs: complex fractionated atrial electrograms.

Panels B–G: ***Off-line analysis of electrograms from dispersion areas and from non-dispersed regions****; comparison between dispersion areas (red), dispersion areas at which AF terminated (red, shaded T) and non-dispersed regions (blue).* **Panel E:** Cycle length. **Panel F:** Voltage amplitude **Panel G:** Rotations**. Panel H:** Presence of continuous CFAEs. **Panel I:** Duration spatio-temporal dispersion/2.5 sec. **Panel J:** Ratio spatio-temporal dispersion/ AFCL. Mean + SE; *: p<0.05; ***: P<0.01; +++ p: <0.05 (Kruskal-Wallis), n = 20 patients; n = 68 and n = 35 dispersion areas and non-dispersed regions, respectively.

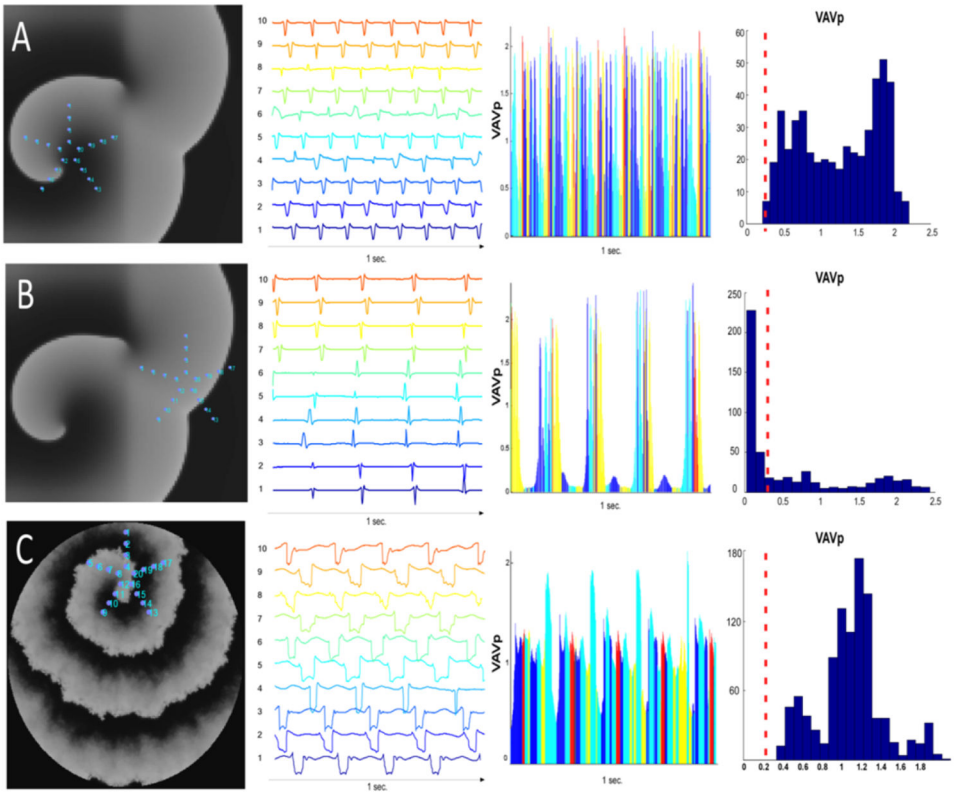

Figure 7. Numerical Simulations

Panel A: Human atrial model, homogeneous substrate: the virtual PentaRay is positioned at the center of the driver. The aspect of the pseudo-multipolar electrograms is one of spatio-temporal dispersion, reminiscent of patients' dispersion areas. **Panel B:** Human atrial model, homogeneous substrate: The virtual PentaRay is positioned at the periphery of the driver in a region activated at a slow frequency of excitation. **Panel C:** Interstitial fibrosis condition (myocyte-myofibroblast ratio: 0.5). The pseudo-multipolar electrograms exhibit a *large* spatio-temporal dispersion. See also supplemental movies 1 and 2. The VAVmax amongst the 10 pseudo-bipoles of the virtual Pentarray was collected at each time point to form a new time-series VAVp. Histograms of the distribution of VAVp values are presented in bins of 0.1 mV. Low VaVp values are underrepresented in the driver regions while they are predominant in bystander regions (red dashed line).

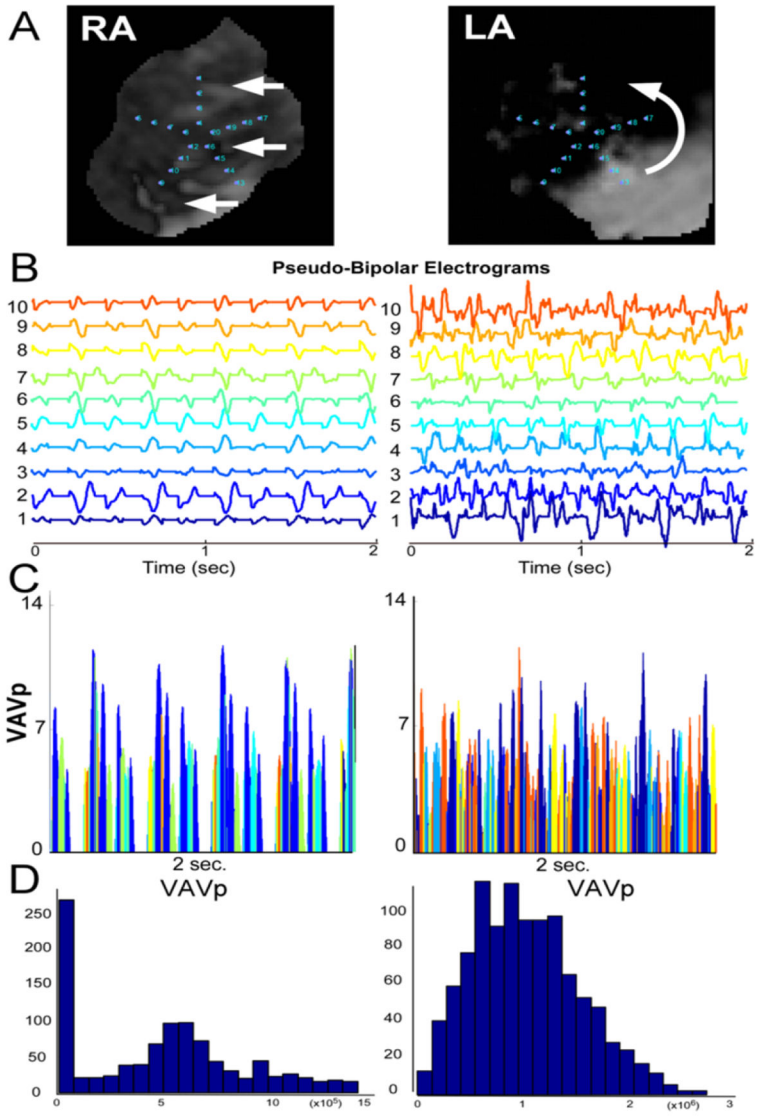

Figure 8. Optical Mapping

Pseudo-multipolar single-pixel time series obtained from an optical mapping experiment in a left--atrial-scar heart. In the RA, planar-like waves yield little tempo-spatial dispersion (RA, left panels). In regards of a LA driver (right panels), however, aspects reminiscent of patients' spatio-temporal dispersion are seen (see also supplemental movie 2). **Panel A:** Optical movie snapshots during AF. **Panel B:** Pseudo-bipolar electrograms. **Panel C:** VAVp time series. **Panel D:** Histograms of the distribution of VAVp values. VAVp: see legend of Figure 7. Low VaVp values are underrepresented in the driver region (LA) while they are predominant in the RA bystander region.

Table 1

Baseline patient characteristics of the study population and the validation set: values are expressed as n (%), mean ± standard deviation.
(AF: atrial fibrillation; LA: left atrial; LVEF: left ventricular ejection fraction.)

	Study population (n=105)	Validation set (n=47)	p
Age (years), mean + SD	63 +11	58±11	0.0046
Male, n (%)	80 (76.2%)	35 (74%)	0.8191
AF type			
Paroxysmal AF, n (%)	24 (22.8%)	9 (19,2%)	0,6
Non-paroxysmal AF, n (%)	81 (77,2%)	38(80,8%)	0,6
Maximum sustained AF duration (months), mean + SD	12.2 + 20	19.4±31.6	0.2457
Structural heart disease, n(%)	38 (36%)	14 (35%)	0.4665
Hypertension, %	48(45,7%)	20 (42,5%)	0.5217
Diabetes, %	13(12.4%)	5(10,6%)	0,5995
LA diameter (mm), mean + SD	45,6± 7,6	42,4±12,4	0,09
LVEF (%), median mean + SD	52 ± 11	54 ± 12	0,2082
Amiodarone before ablation, %	32%	NA	
Spontaneous AF at the beginning of procedure (persistent and longstanding persistent AF only), n	65	NA	

Table 2

Surface area of dispersion regions and of regions ablated (n=43 patients).

	All patients	Paroxysmal (n=15)	Persistent (n=17)	LS-Persistent (n=11)	p
Dispersion areas					
Total dispersion areas surface (cm^2), mean ± SD, median [Q1–Q3]	22.5±13.5 19[12.5–33]	18 ±10 4.5 17 [13–22]	17±9 15 [11–19]	41±12 40 [32–50]	<.0001
Mean dispersion areas surface (cm^2), mean ± SD, mean ± SD, median [Q1–Q3]	5±2 4.5[3–6]	5±2 4.5 [3.4–6.0]	4±1.5 3.2[2.9–5.6]	6±2 6.0 [4.9–8.2]	0.0025
Number of dispersion areas, mean ± SD, median [Q1–Q3]	5±1.5 5[4–6]	4±1.7 4 [3–5]	5±1.2 5 [4–5]	6±1 6 [5–7]	0.02
Ablation in the RA RA Ablated surface (cm^2), mean ± SD, median [Q1–Q3]	6±5 4.5[2–7]	4±5 3 [0–4]	5±3 5 [2–6]	9±7 7 [4–15]	0.03
RA total surface (cm^2), mean ± SD, median[Q1–Q3]	154±58 150[122–184]	138.3±71.0 129[121–186]	138.9±36.5 135[117–169]	196.5±50.2 186[167–220]	0.003
% of RA Ablated surface, mean ± SD	4±2.5	3.8±3	4.2±3	4.0±2.5	0.9
Ablation in the LA					
LA Ablated surface (cm^2), mean ± SD, median [Q1–Q3]	25.5±15.7 20.6 [15–35.5]	20.5±10.5 19 [14–27]	16.5±6 17 [11–21]	46±13.5 40 [36–56]	<.0001
LA total surface (cm^2), mean ± SD, median[Q1–Q3]	157±47 156 [135–171]	139±44 153[114–164]	167±53 156[135–172]	165.5±35 165[152–175]	0.18
% of LA Ablated surface, mean ± SD	17±10	15.8±8.8	10.1±4.0	29±9.7	<.0001
Ablation in both atria					
Biatrial total surface (cm^2), mean ± SD, median[Q1–Q3]	302±85 312 [257–350]	266±97.5 288[207–331]	296±53 293[273–322]	361±82.5 340[320–398]	0.06
Biatrial Total Ablated surface (cm^2), mean ± SD, median [Q1–Q3]	31±19 24.5 [18–39.5]	25±12 21 [17–39]	21±7.0 20 [16–23]	55±17.5 50 [42–74]	<.0001
% of biatrial Ablated surface (cm^2), mean ± SD	10±5	10±4	7.5±2.5	15±4	0.0005

LA: left atrium

LS-Persistent: Long standing-Persistent

RA: right atrium

Values are expressed as n (%), mean ± standard deviation (SD), median [Q1–Q3].

Table 3

Distribution of dispersion areas. For each atrial sub-region, the percentage indicates the proportion of patients in whom we counted at least one dispersion area.

Regions	Dispersion Areas (% of patients)
Left pulmonary veins and left appendage	**79%**
Right pulmonary veins and posterior interatrial groove	**78%**
Inferior and posterior left atrium	**73%**
Upper half of right atrium and appendage	**42%**
Lower half of right atrium	**31%**
Anterior left atrium and roof	**77%**
Anterior interatrial groove	**77%**

Table 4

Per-Procedural Outcome (Index and Redo Procedures)

	Rhythm	Procedure Time (min)	RF Time (min)	Fluoroscopic Time (min)	Sinus Rhythm Conversion	Non inducibility Tested and Obtained
Ablation procedure # 1 (n = 105)	AF = 100%	168 ± 42	49 ± 21	15 ± 13	77%	42%
Ablation procedure # 2 (n = 38)	AF = 24% (AT = 76%)	125 ± 43 *	27 ± 21 *	10 ±10 *	85%	64%
Ablation procedure # 3 (n = 3)	AF = 33% (AT = 67%)	109 ± 8 *	17.5 ± 10 *	7 ± 4 *	100%	100%

Values are mean ± SD OR%.

* $p < 0.005$.